Volume 22
Number 8
April 13, 1983

Inorganic Chemistry

Contribution No. 6671 from the Arthur Amos Noyes Laboratory of Chemical Physics,
California Institute of Technology, Pasadena, California 91125

X-ray Crystal Structure Determination of $[\eta^5\text{-}C_5(CH_3)_5]Ta[P(CH_3)_3]_2H_4$ and High-Field NMR Studies of Phosphine Derivatives of (Pentamethylcyclopentadienyl)tantalum(V) Hydrides

JAMES M. MAYER,[1] PETER T. WOLCZANSKI, BERNARD D. SANTARSIERO,[2] WENDY A. OLSON,[3] and JOHN E. BERCAW*[4]

Received June 29, 1982

Low-temperature and high-field NMR spectra have been obtained for a number of niobium and tantalum polyhydride complexes, $(\eta^5\text{-}C_5Me_5)ML_2H_3X$ (X = H, L = PMe_3, $P(OMe)_3$, L_2 = dmpe, M = Nb, Ta; X = Cl, L = PMe_3, M = Ta). The coordination geometries of these molecules have been determined from the spectra with the use of symmetry arguments. A structure with C_s symmetry and equivalent phosphorus atoms is indicated for complexes with monodentate phosphine ligands; this is consistent with an X-ray crystal structure determination of $(\eta^5\text{-}C_5Me_5)Ta(PMe_3)_2H_4$, in which all but the hydride ligands were located. The following data were obtained: $TaP_2C_{16}H_{37}$, $P\bar{1}$, a = 8.581 (2) Å, b = 14.244 (4) Å, c = 17.267 (14) Å, α = 90.34 (2)°, β = 99.96 (2)°, γ = 90.05 (2)°, Z = 4. A different C_s structure, with inequivalent phosphorus atoms, is indicated for compounds with the bidentate dmpe ligand. The synthesis and spectra of a new dimeric tantalum alkoxide hydride compound are also reported. The NMR data are indicative of an unusual asymmetric structure: $(\eta^5\text{-}C_5Me_5)(Me_3CO)_2HTa(\mu\text{-}H)_2TaH_3(\eta^5\text{-}C_5Me_5)$.

Introduction

The structural characterization of molecules with high coordination numbers is of considerable interest, and transition-metal complexes with a number of hydride ligands are among the most common and sterically least crowded examples of eight- and nine-coordinate complexes.[5-7] The determination of these structures is complicated by the difficulties in locating hydrogen atoms by X-ray diffraction, principally owing to the low scattering efficiency of the hydrogen atom.[7,8] The hydrogen atom positions of many structures have often been inferred from the orientation of the remaining ligands, but this is unreliable for polyhydride complexes lacking high crystallographic site symmetry.[8] Neutron diffraction studies would, of course, be more useful, since the hydrogen atoms are precisely located, but at present experimental difficulties prevent routine use.[7] NMR spectra have been used to establish stoichiometries and occasionally coordination geometries;[9] however, fluxional processes are common in these molecules, and static structures are rarely observed.[9] In addition, the spectra often show complex overlapping patterns, particularly when $^{31}P\text{-}^1H$ coupling is present. A very high-field NMR spectrometer offers obvious advantages in these regards. Thus, we have utilized the 500-MHz NMR spectrometer at the NSF Southern California Regional NMR Facility to obtain the NMR spectra of a series of niobium and tantalum hydride complexes, $Cp^*ML_2H_3X$ (Cp^* = $\eta^5\text{-}C_5Me_5$; X = H, L = PMe_3, $P(OMe)_3$, L_2 = dmpe, M = Nb, Ta, and X = Cl, L = PMe_3, M = Ta).[10] Starting from the heavy-atom structure of $Cp^*Ta(PMe_3)_2H_4$ (**1**) determined from single-crystal X-ray diffraction data, we have used NMR data to elucidate the structures of these compounds. The synthesis of the new tantalum hydride complex $Cp^*_2Ta_2H_6(OCMe_3)_2$ is also reported, and the NMR spectra indicate a novel asymmetric structure.

Description of the Structure

Figure 1 depicts one of the two crystallographically independent molecules found in the structure of $Cp^*Ta(PMe_3)_2H_4$ (**1**), along with the atom-labeling scheme. There are no short intra- or intermolecular contacts. The hydride ligands were not located; their positions are discussed with the NMR spectra, below. The two independent molecules have very similar coordination geometries (see Figure 9, supplementary material) with statistically equivalent bond lengths and angles. The only exception is the pair of phosphorus–tantalum–phosphorus angles, which are statistically although not substantially different, 116.0 and 112.3 (1)°. In discussing the structure of **1**, we have used average values for all bond lengths and angles.

The pentamethylcyclopentadienyl ring is coordinated in the conventional η^5 manner with Ta–C bond lengths from 2.39 to 2.46 Å (Table I); the average (2.42 Å) is within the range

---

[1] National Science Foundation Predoctoral Fellow, 1978–1981.

[2] Myron A. Bantrell Fellow, 1981–1983.

[3] National Science Foundation Fellow, 1980–1983.

[4] Camille and Henry Dreyfus Teacher-Scholar, 1977–1982.

[5] (a) Muetterties, E. L., Ed. "Transition Metal Hydrides"; Marcel Dekker: New York, 1971. (b) Bau, R., Ed. "Transition Metal Hydrides"; American Chemical Society: Washington, DC, 1978; Adv. Chem. Ser. No. 167. (c) Kaesz, H. D.; Saillant, R. B. *Chem. Rev.* **1972**, *72*, 231.

[6] Meakin, P.; Guggenberger, L. J.; Peet, W. G.; Muetterties, E. L.; Jesson, J. P. *J. Am. Chem. Soc.* **1973**, *95*, 1467–74.

[7] Teller, R. G.; Bau, R. *Struct. Bonding (Berlin)* **1981**, *44*, 1–82.

[8] (a) Frenz, B. A.; Ibers, J. A. In ref 5a, pp 33–74. (b) Ibers, J. A. In ref 5b, pp 26–35.

[9] Jesson, J. P. In ref 5a, pp 75–201.

[10] (a) Mayer, J. M.; Bercaw, J. E. *J. Am. Chem. Soc.* **1982**, *104*, 2157–65. (b) Olson, W. A.; Bercaw, J. E., work in progress.

0020-1669/83/1322-1149$01.50/0 © 1983 American Chemical Society

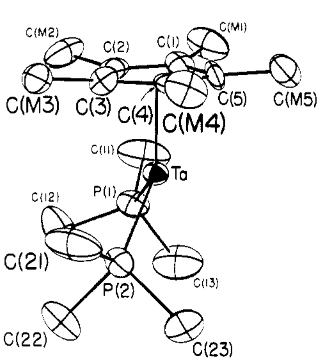

Figure 1. ORTEP drawing of $Cp^*Ta(PMe_3)_2H_4$ (**1**, molecule 1). The hydrogen atoms have been omitted for clarity.

Table I. Important Distances and Angles in the Structure of $Cp^*Ta(PMe_3)_2H_4$[a]

	molecule A	molecule B	av[b]
	Distances and Angles		
Ta-P(1)	2.534 (5)	2.528 (5)	2.532 (3)
Ta-P(2)	2.529 (5)	2.535 (5)	
Ta-C(1)	2.454 (15)	2.460 (17)	2.42 (3)
Ta-C(2)	2.400 (17)	2.433 (15)	
Ta-C(3)	2.425 (17)	2.388 (17)	
Ta-C(4)	2.404 (18)	2.424 (17)	
Ta-C(5)	2.387 (16)	2.441 (16)	
P(1)-Ta-P(2)	116.1 (2)	112.4 (2)	114 (3)
R-Ta-P(1)[c]	117.1 (1)	120.4 (1)	119 (2)
R-Ta-P(2)	117.5 (1)	119.8 (1)	
P(1)-C(11)	1.85 (2)	1.80 (2)	1.82 (3)
P(1)-C(12)	1.78 (2)	1.82 (2)	
P(1)-C(13)	1.80 (2)	1.81 (2)	
P(2)-C(21)	1.81 (2)	1.80 (2)	
P(2)-C(22)	1.85 (2)	1.82 (2)	
P(2)-C(23)	1.82 (2)	1.87 (2)	
C(11)-P(1)-C(12)	99.7 (11)	99.9 (11)	99 (2)
C(11)-P(1)-C(13)	96.6 (11)	96.1 (11)	
C(12)-P(1)-C(13)	101.2 (11)	100.7 (11)	
C(21)-P(2)-C(22)	100.9 (9)	98.3 (10)	
C(21)-P(2)-C(23)	103.3 (9)	100.2 (10)	
C(22)-P(2)-C(23)	98.1 (9)	98.1 (9)	
C(1)-C(2)	1.39 (2)	1.46 (2)	1.42 (2)
C(2)-C(3)	1.40 (2)	1.41 (2)	
C(3)-C(4)	1.44 (2)	1.44 (2)	
C(4)-C(5)	1.43 (2)	1.39 (2)	
C(5)-C(1)	1.39 (2)	1.42 (2)	
	Displacement from Least-Squares Cp* Ring Plane[d]		
C(M1)	0.23	0.18	0.20 (5)
C(M2)	0.19	0.18	
C(M3)	0.28	0.19	
C(M4)	0.22	0.23	
C(M5)	0.16	0.10	

[a] Distances are given in Å and angles in degrees. Estimated standard deviations are indicated in parentheses. [b] The standard deviation of the average is estimated as $[\Sigma_{i=1}^{n}(d_i - \bar{d})^2/(n-1)]^{1/2}$. [c] R = Cp* ring centroid. [d] The least-squares plane was determined with the five ring carbon atoms; displacements are given in Å.

found for other TaCp* complexes.[11] As expected, the ring is planar (the maximum displacement is about 0.02 Å) and the methyl carbon atoms are each displaced from the ring by about 0.20 Å in a direction away from the Ta center. The tantalum–phosphorus bond lengths are the same (average 2.532 (3) Å) and within the range of $Ta-PMe_3$ distances previously observed (2.51–2.60 Å).[11a,12] The phosphorus–carbon bond lengths are normal, 1.78–1.85 (2) Å, and the CH_3P-CH_3 angles are all less than the tetrahedral value of 109° (average 99°). The two ring-centroid–tantalum–phosphorus angles are essentially the same (119°). There is a distinct asymmetry in the coordination geometry, however, since the point midway between the phosphorus nuclei is not directly opposite the Cp* ring: the ring-centroid–tantalum–PP-midpoint angle is 153°. Thus, the hydride ligands significantly influence the stereochemistry of the remaining ligands and appear to be somewhat asymmetrically disposed.

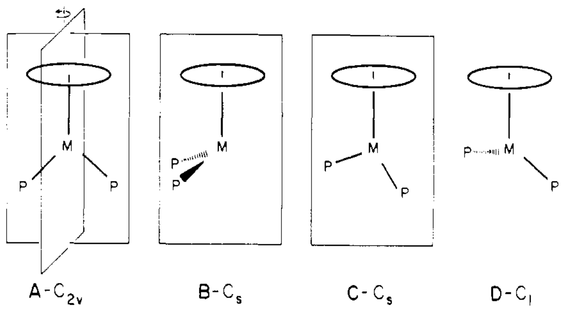

Figure 2. Possible geometries for a Cp^*ML_2 fragment. The Cp* ligand is represented as an ellipse.

NMR Studies

General Considerations. The determination of structures of organometallic complexes by NMR spectroscopy is in general not a straightforward procedure. Only for very well-defined coordination geometries, like octahedral and square-planar arrangements, can the stereochemistry be assigned simply from the number and multiplicity of the resonances.[9] The NMR data have been interpreted without assuming any particular coordination geometry. In most cases, the spectra provide sufficient information to determine the point group of the molecule and the disposition of the ligands with respect to the symmetry element(s). The NMR spectral analysis requires only the assumption that there are no accidental degeneracies in the spectra. Since the spectra are obtained at high field, degeneracies are particularly unlikely, especially for the resonances that are complex multiplets, where fortuitous equivalence of both chemical shifts and coupling constants would be required.[13]

The compounds examined in this study are eight- or nine-coordinate, considering a cyclopentadienyl ring as formally occupying three sites. In view of the small energy differences between the various geometries for these coordination numbers and the low barriers for their interconversion,[14] it is not surprising that the compounds are found to be highly fluxional at ambient temperatures. In addition, complexes with hydride ligands tend to have smaller barriers for rearrangement processes.[6,9,15] The use of low-temperature, high-field NMR spectroscopy provides favorable conditions for the observation of static structures.[16] Relatively sharp spectra are observed

---

(11) (a) Schulz, A. J.; Brown, R. K.; Williams, J. M.; Schrock, R. R. *J. Am. Chem. Soc.* **1981**, *103*, 169–76. (b) McLain, S. J.; Wood, C. D.; Messerle, L. W.; Schrock, R. R.; Hollander, F. J.; Youngs, W. J.; Churchill, M. R. *Ibid.* **1978**, *100*, 5962–64. (c) Messerle, L. W.; Jennische, P.; Schrock, R. R.; Stucky, G. *Ibid.* **1980**, *102*, 6744–52. (d) Churchill, M. L.; Youngs, W. J. *Ibid.* **1979**, *101*, 6462–3. (e) Churchill, M. L.; Youngs, W. J. *Inorg. Chem.* **1979**, *18*, 1697–1702. (f) Smith, G.; Schrock, R. R.; Churchill, M. R.; Youngs, W. J. *Ibid.* **1981**, *20*, 387–93.

(12) (a) Churchill, M. R.; Youngs, W. J. *Inorg. Chem.* **1979**, *18*, 171–6. (b) *Ibid.* **1979**, *18*, 1930–5.

(13) Accidental degeneracies in the ^{31}P NMR spectra are unlikely due to the sensitivity of phosphorus chemical shifts to small changes in environment. Also, the proton NMR spectra of the alkyl groups on the phosphine ligands provide an independent measure of the equivalence of the phosphorus nuclei.

(14) (a) Muetterties, E. L. *Rec. Chem. Prog.* **1970**, *31*, 51–88. (b) Drew, M. G. B. *Coord. Chem. Rev.* **1977**, *24*, 179–275.

(15) Gerlach, D. H.; Peet, W. G.; Muetterties, E. L. *J. Am. Chem. Soc.* **1972**, *94*, 4545–9.

(16) Even under these conditions, however, some fluxional processes are still active, for example, the rotation of the cyclopentadienyl ring.

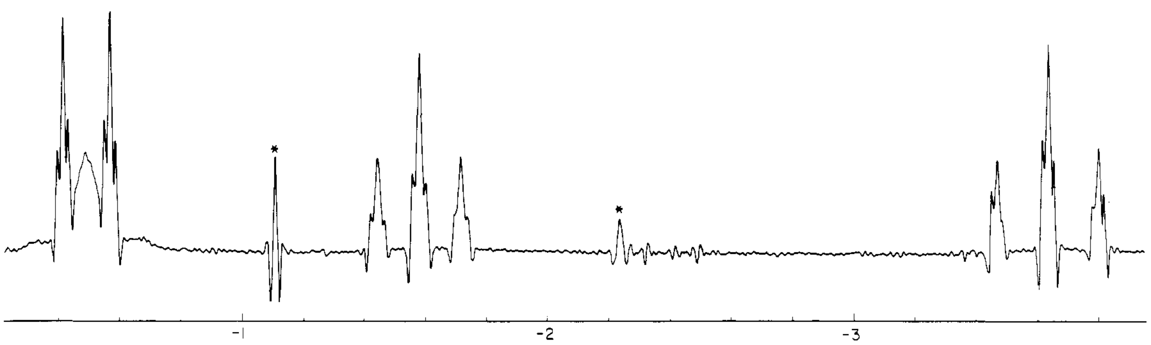

Figure 3. Hydride region of the 500-MHz ^1H NMR spectrum of $Cp^*Ta[P(OMe)_3]_2H_4$ at −70 °C. Asterisks denote impurity resonances. The spectrum is resolution enhanced.

and are taken as indicative of ground-state structures. Thus we assume that the degeneracies observed in the low-temperature NMR spectra are indicative of a symmetry element of the molecule that requires the rigorous equivalence of the nuclei involved, not of a fluxional process with an extremely low energy barrier.

Compounds of the Type $Cp^*ML_2H_3X$. The ^1H NMR spectrum for each member of the series $Cp^*ML_2H_4$ (M = Ta, L = PMe_3, $P(OMe)_3$, L_2 = dmpe; M = Nb, L = PMe_3, L_2 = dmpe) exhibits a single binomial triplet for the four hydride ligands at ambient temperatures.[10] As the temperature is lowered, the hydride signals broaden and give rise to more complex patterns. With the assumptions above the spectra may be interpreted without reference to the crystal structure of **1**. In each case the geometry of the Cp^*ML_2 fragment is first determined and then the positions of the hydride ligands are considered. From a symmetry standpoint, there are only four possible arrangements for a Cp^*ML_2 group (Figure 2): one with C_{2v} symmetry (A), two structures with C_s symmetry (B and C), and one with C_1 symmetry (D).[17]

The trimethyl phosphite groups in $Cp^*Ta[P(OMe)_3]_2H_4$ (**2**) are equivalent in the low-temperature limit by both phosphorus and proton NMR spectroscopy, so that only structures A and B need be considered as "frames" on which to place the hydride ligands. The hydride region of the low-temperature proton NMR spectrum of **2** (Figure 3) exhibits three multiplets in which the large splittings are due to phosphorus–hydrogen coupling and the small splittings are due to coupling between the hydride ligands; integration yields a 2:1:1 ratio. A C_{2v} geometry (A) for the complex is inconsistent with the integration because with this symmetry a ligand must lie on the twofold axis in order to be unique, i.e. in order not to have a symmetry-generated partner, and in A only one coordination site is available (trans to the Cp*) for a unique hydride ligand. The C_s geometry of B is consistent if the two magnetically equivalent hydride ligands (H_a) are related to each other by the mirror plane and the two unique hydrides (H_b and H_c) are located in the mirror plane. Furthermore, as a result of this geometry H_b and H_c would generate an AX_2 pattern (a binomial triplet) and the two H_a ligands a more complex AA′XX′ pattern, as observed in the spectrum.

Ideally, this structure can be envisioned as a tricapped trigonal prism (Figure 4a) with the Cp* ring at one triangular face, the two phosphite ligands and one hydride ligand generating the opposite face. The remaining hydride ligands would occupy the three capping sites.[18] This idealized ge-

Table II. NMR Data for $Cp^*ML_2H_3X$ Compounds[a]

compd	chem shift		P-H coupling	H-H coupling
$Cp^*Ta(PMe_3)_2H_4$ (**1**)	1 H_a	0.32	t, $J_{PH} = 64$	*b*
	1 H_b	0.35	t, $J_{PH} = 78$	
	2 H_c	~1.4	m	
$Cp^*Ta[P(OMe)_3]_2H_4$ (**2**)	1 H_a	−3.63	t, $J_{PH} = 82$	$J_{H_aH_b} < 3^d$
	1 H_b	−1.58	t, $J_{PH} = 68$	$J_{H_aH_c} = 9$
	2 H_c	−0.50	$J_{PH} \simeq 38^c$	$J_{H_bH_c} = 12$
$Cp^*Nb(PMe_3)_2H_4$ (**3**)	1 H_a	−3.05	t, $J_{PH} = 78$	*b*
	1 H_b	−1.24	t, $J_{PH} = 76$	
	2 H_c	−0.93	broad s^e	
$Cp^*Ta(PMe_3)_2H_3Cl$ (**4**)	1 H_a	5.29	t, $J_{PH} = 68$	$J_{HH} = 10$
	2 H_b	4.67	dm, $J_{PH} = 72$, $J_{P'H} \simeq 15^c$	
$Cp^*Ta(dmpe)H_4$ (**5**)	2 H_a	−0.51	dd, $J_{PH} = 53$, $J_{P'H} = 28$	$J_{HH} = 9$
	2 H_b	0.52	dd, $J_{PH} = 49$, $J_{P'H} = 15$	
$Cp^*Nb(dmpe)H_4$ (**6**)	2 H_a	−1.77	t, $J_{PH} = 47$	*b*
	2 H_b	−1.10	m^f	

^{31}P NMR

$Cp^*Ta(PMe_3)_2H_4$ (**1**), $Cp^*Ta[P(OMe_3)]_2H_4$ (**2**), $Cp^*Nb(PMe_3)_2H_4$ (**3**), and $Cp^*Ta(PMe_3)_2H_3Cl$ (**4**): one singlet over the range 25 to −90 °C

$Cp^*Ta(dmpe)H_4$ (**5**): singlet at 25 °C and a pair of doublets at −80 °C ($|\delta_P - \delta_{P'}| = 0.75$, $J_{PP'} = 18$ Hz; coalescence temperature −45 °C)

$Cp^*Nb(dmpe)H_4$ (**6**): singlet at 25 °C and pair of doublets at −90 °C ($|\delta_P - \delta_{P'}| = 0.52$, $J_{PP'} = 34$ Hz; coalescence temperature −80 °C)

[a] Spectra in toluene-d_8 solvent at −70 °C except as noted. Proton NMR spectra were obtained at 500 MHz and were frequently resolution enhanced to observe small coupling constants; only the resonances due to hydride ligands are reported. Assignments are ambiguous except where determined by integration. Chemical shifts are reported in δ, referenced to signals due to residual protons in the solvent; coupling constants are in hertz. Phosphorus spectra were obtained at 36.21 MHz and are proton decoupled. Ambient-temperature spectra of the tantalum compounds are given in ref 10a. [b] Hydrogen-hydrogen coupling is not resolved due to broad resonances. [c] Non-first-order NMR pattern; coupling constants are those that best describe the pattern (see Figure 4 or 6). [d] Coupling not observed. Limits given are based on estimates of the resolution in the spectrum. [e] 150-Hz full width half-height. [f] Broad complex pattern, 70-Hz width.

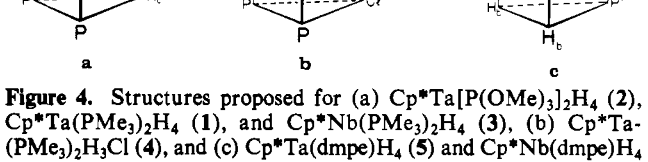

Figure 4. Structures proposed for (a) $Cp^*Ta[P(OMe)_3]_2H_4$ (**2**), $Cp^*Ta(PMe_3)_2H_4$ (**1**), and $Cp^*Nb(PMe_3)_2H_4$ (**3**), (b) $Cp^*Ta(PMe_3)_2H_3Cl$ (**4**), and (c) $Cp^*Ta(dmpe)H_4$ (**5**) and $Cp^*Nb(dmpe)H_4$ (**6**). The Cp* ligand is represented as a shaded triangle in these drawings.

---

(17) The Cp* ligand is assumed to be axially symmetric in these structures.[16] It is also possible to obtain a structure with C_2 symmetry, by adding the hydride ligands asymmetrically to the C_{2v} geometry. However, this configuration can easily be ruled out for the molecules discussed.

(18) Although a related structure for **1**–**4** with H_b capping the triangular face (opposite Cp*) cannot be excluded, we prefer the more plausible (on steric grounds) structure with H_b capping the rectangular face, as shown in Figure 5.

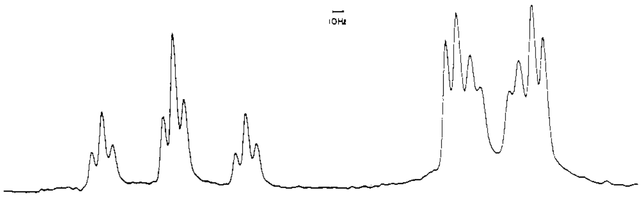

Figure 5. Hydride region of the 500-MHz ^1H NMR spectrum of $Cp^*Ta(PMe_3)_2H_3Cl$ (**4**) at -70 °C. The spectrum is resolution enhanced.

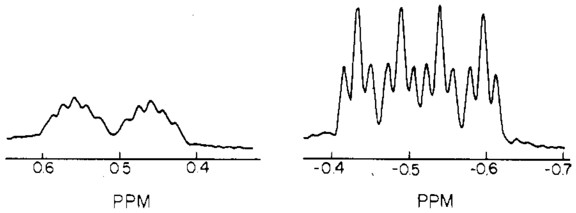

Figure 6. Resonances due to the hydride ligands in the 500-MHz ^1H NMR spectrum of $Cp^*Ta(dmpe)H_4$ (**5**) at -70 °C. The spectrum is resolution enhanced. The two resonances are not plotted on the same vertical scale.

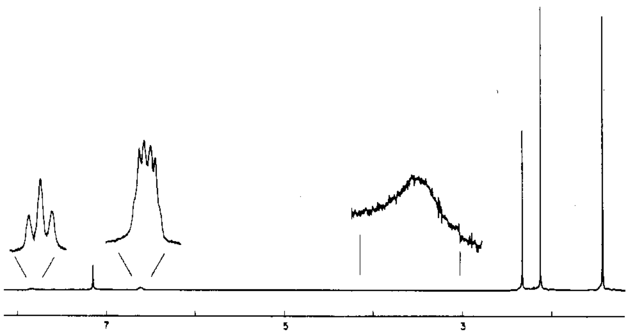

Figure 7. 500-MHz ^1H NMR spectrum of $Cp^*(Me_3O)_2HTa(\mu\text{-}H)_2TaH_3Cp^*$ (**7**) at 25 °C. The resonance at δ 7.15 is due to residual protons in the benzene-d_6 solvent.

ometry is the most common arrangement observed for nine-coordinate complexes,[14] e.g., ReH_9^{2-}.[19] The actual structure of **2** is expected to be significantly distorted from the idealized geometry, however, considering the variety of ligands involved.[20]

The structures of $Cp^*Ta(PMe_3)_2H_4$ (**1**) and $Cp^*Nb(PMe_3)_2H_4$ (**3**) are similar to the one described above, as indicated by the analysis of the low-temperature NMR spectra. For both **1** and **3** the phosphine ligands are magnetically equivalent and the hydride resonances appear in a 2:1:1 ratio, although they are not well resolved. If only the coordination sphere is considered, the NMR analysis is consistent with the crystal structure of **1**. Whereas the trimethylphosphine ligands are not crystallographically equivalent in the solid-state structure, the Cp* ring, Ta and P atoms do closely approach the idealized geometry B. Once again, the structure can be based on a trigonal prism, although the phosphorus–tantalum–phosphorus angle (114°) is considerably larger than that predicted for the (squared-faced) idealized geometry (82°). The tricapped-trigonal-prism geometry (Figure 4a), derived from the NMR analysis, places H_b in the cavity created by the Cp* ring and the methyl groups of the PMe_3 ligands (see Figure 1) and places H_c also on the pseudo mirror plane, on the opposite side of the phosphorus atoms.

$Cp^*Ta(PMe_3)_2H_3Cl$ (**4**) seems to have the same basic geometry (Figure 4b). The NMR spectra again indicate equivalent phosphine ligands in the low-temperature limit and two multiplets of intensity 1:2 for the hydride ligands (Figure 5). The proposed structure is consistent with the resonance for the single hydrogen (H_b) being a first-order triplet of triplets and the pair of equivalent hydrogen atoms (H_a) being a complex AA′MXX′ pattern. Interestingly, in contrast to the case of the highly fluxional tetrahydride compounds **1**, **2**, and **3**, the hydride ligands in **4** are inequivalent at room temperature on the NMR time scale,[10] a very rare occurrence for polyhydride complexes of nonoctahedral geometry.[9] Moreover, the phosphine ligands in **4** are labile, again unlike **1**–**3**, undergoing a rapid reversible dissociation at ambient temperatures (eq 1). Hence, the resultant 16-electron species I must also be static on the NMR time scale.

$$Cp^*Ta(PMe_3)_2H_3Cl \rightleftharpoons \underset{\text{I}}{[Cp^*Ta(PMe_3)H_3Cl]} + PMe_3 \quad (1)$$

A different type of structure is adopted by the two complexes with the bidentate dmpe ligand, $Cp^*Ta(dmpe)H_4$ (**5**) and $Cp^*Nb(dmpe)H_4$ (**6**). The low-temperature $^{31}P\{^1H\}$ spectra for these compounds exhibit AB patterns, and the hydride ligands appear in the low-temperature proton spectra as two multiplets (Figure 6), each integrating as two hydrogen atoms. The inequivalence of the phosphorus atoms rules out skeletal geometries A and B, and the pairwise equivalence of the hydride ligands implies a plane of symmetry. The C_s skeletal geometry C is indicated, with the two phosphorus nuclei in the mirror plane and each pair of hydride ligands related by the mirror plane. This geometry can also be derived from a tricapped trigonal prism, with the Cp* group spanning two corners of the prism and one capping site (Figure 4c).

It should be emphasized that the NMR data are *not* consistent with a structure for **5** and **6** that resembles the one found for the complexes of monodentate phosphine ligands. The reasons for this structural difference are not obvious. Electronically, the complexes are very similar and the d^0 metal center could be expected to have small intrinsic geometrical preferences. An argument based on overall steric crowding is unlikely, since the cone angle of dmpe is roughly the same as that of two $P(OMe)_3$ groups.[21] Further, $Cp^*Ta[P(OMe)_3]_2H_4$ adopts the same basic geometry as $Cp^*Ta(PMe_3)_2H_3Cl$, the most sterically crowded molecule in the series. There are structures in which the dmpe ligand does adopt the geometry found here for the complexes of monodentate phosphines, e.g. $Cp^*Ta(dmpe)(CO)_2$, which has a "four-legged piano stool" type of geometry (by NMR spectroscopy).[10] The small bite angle of the dmpe ligand (75°[22]), relative to that preferred in the case of PMe_3 (114°), is undoubtedly an important factor in determining the preferred structure.

[$Cp^*(Me_3CO)_2HTa(\mu\text{-}H)_2TaH_3Cp^*$] (7). High-field NMR spectroscopy has also been of great help in characterizing the new tantalum polyhydride complex **7**. **7** is prepared either by replacement of the chloride ligand in $Cp^*Ta(PMe_3)_2H_3Cl$ (**4**) by *tert*-butoxide or alternatively by substitution of the chloride in Cp^*TaMe_3Cl by $OCMe_3$, followed by high pressure

---

(19) Abrahams, S. C.; Ginsburg, A. P.; Knox, K. *Inorg. Chem.* **1964**, *3*, 558–67.

(20) A similar structure has been postulated for $ReH_7(PMe_2Ph)_2$ on the basis of an X-ray crystallographic study in which the hydride ligands were not located: Bau, R.; Carroll, W. E.; Hart, D. W.; Teller, R. G.; Koetzle, T. F. In ref 5a, pp 73–92.

(21) Tolman, C. A. *Chem. Rev.* **1977**, *77*, 313–348.

(22) Phosphorus–tantalum–phosphorus angles in the range 74–78° have been found in the following five crystal structures of Ta–dmpe complexes: (a) Domaille, P. J.; Foxman, B. M.; McNeese, T. J.; Wreford, S. S. *J. Am. Chem. Soc.* **1980**, *102*, 4114–20. (b) Allright, J. O.; Datta, S.; Dezube, B.; Kouba, J. K.; Marynick, D. S.; Wreford, S. S.; Foxman, B. M. *Ibid.* **1979**, *101*, 611–619. (c) Foxman, B. M.; McNeese, T. J.; Wreford, S. S. *Inorg. Chem.* **1978**, *17*, 2311–2314. (d) Meakin, P.; Guggenberger, L. J.; Tebbe, F. N.; Jesson, J. P. *Ibid.* **1974**, *13*, 1025–32. (e) McNeese, T. J.; Wreford, S. S.; Foxman, B. M. *J. Chem. Soc., Chem. Commun.* **1978**, 500–1.

$$\begin{tikzcd}
Cp^{*}TaMe_3Cl \arrow[r, "2PMe_3,\ H_2\ (100\ atm)"] \arrow[d, "KOCMe_3"] & \underset{\mathbf{4}}{Cp^{*}Ta(PMe_3)_2H_3Cl} \arrow[d, "KOCMe_3"] \\
Cp^{*}TaMe_3(OCMe_3) \arrow[r, "PMe_3,\ H_2\ (100\ atm)"] & \underset{\mathbf{7}}{[Cp^{*}TaH_3(OCMe_3)]_2}
\end{tikzcd}$$

hydrogenation of $Cp^{*}TaMe_3(OCMe_3)$ at 65 °C. Due to its extreme solubility in hydrocarbon solvents, **7** is difficult to isolate. Whereas the hydrogenation reaction does not require trimethylphosphine, the product appears to be slightly cleaner if a stoichiometric amount of PMe_3 is added. Its elemental analysis supports an empirical formula of $Cp^{*}TaH_3(OCMe_3)$, and the molecular weight indicates a dimeric structure for **7** (calcd 785, found 760).

The 500-MHz proton NMR spectrum of **7** at 25 °C (Figure 7, Table III) shows three large singlets at δ 2.32, 2.12, and 1.42, and integration gives a 5:5:6 ratio. The first two singlets are assigned to two inequivalent Cp* ligands, and the third singlet is ascribed to two equivalent *tert*-butoxide groups. The inequivalence of the Cp* rings indicates that the tantalum atoms are inequivalent, forcing the surprising conclusion that both alkoxide groups must be bound to one of the tantalum atoms. The spectrum also shows resonances assignable to hydride ligands: a triplet at δ 7.84 (J_{HH} = 13 Hz, 1 H), a doublet of quartets at δ 6.62 (J_{HH} = 13, 6 Hz, 2 H) and a very broad peak at δ 3.5 (J = 250 Hz full width half-height, 3 H). The resonance at δ 6.62 collapses to a doublet (J = 13 Hz) on selective decoupling at δ 3.5, but the triplet at δ 7.84 is unaffected. Since coupling is usually observed between inequivalent hydride ligands on the same metal center,[9] the hydride at δ 7.84 and the group of three hydride ligands at δ 3.5 are expected to be bound to different tantalum atoms. The two hydrogen atoms at δ 6.62 appear to bridge the two tantalum atoms, since they couple to each of the other groups of hydride ligands. This arrangement of hydride ligands forces the same conclusion that both *tert*-butoxide groups are on the same tantalum atom: $Cp^{*}(Me_3CO)_2HTa(\mu\text{-}H)_2TaH_3Cp^{*}$ (Figure 8).[23]

The broad resonance at δ 3.5 separates into two sharp resonances as the sample is cooled from 25 to −70 °C, indicating that the fluxional process involving the three terminal hydride ligands is effectively frozen out. The equivalence of the *tert*-butoxide ligands implies that there is a mirror plane in the molecule[24] containing the unique atoms or groups: the tantalum atoms, ring centroids, and unique hydride ligands. The structure has been drawn (Figure 8) with the bulky ligands (Cp* and $OCMe_3$) far apart and with groups in the plane next to pairs of ligands, a reasonable configuration based on steric interactions.

It is not clear why **7** adopts this geometry rather than the symmetric alternative. The small kinetic barrier for scrambling ligands between metal centers indicates that the arrangement is the thermodynamically most stable configuration.[25] The fact that **7** is synthesized from equivalent monomers also demonstrates the facility of this ligand-exchange process. This asymmetric structure adopted for **7** is all the more surprising considering the fact that a symmetric isomer with either bridging hydrides or bridging *tert*-butoxides could be considered formally closed shell.

Table III. ^1H NMR Data for $Cp^{*}(Me_3CO)_2HTa(\mu\text{-}H)_2TaH_3Cp^{*}$ (**7**)[a]

conditions	chem shift	integral	coupling	assignt
C_6D_6, 25 °C	2.32	15	s	$C_5(CH_3)_5$
	2.12	15	s	$C_5(CH_3)_5$
	1.42	18	s	$[(CH_3)_3CO]_2Ta$
	7.84	1	t, $^2J_{HH}$ = 13 Hz	$\mathit{H}Ta(\mu\text{-}H)_2TaH_3$
	6.62	2	dq, $^2J_{HH}$ = 13, 6 Hz	$HTa(\mu\text{-}\mathit{H})_2TaH_3$
	3.5	3	broad s[b]	$HTa(\mu\text{-}H)_2Ta\mathit{H}_3$
C_7D_8, −70 °C	7.75	1	t, $^2J_{HH}$ = 13 Hz	$\mathit{H}Ta(\mu\text{-}H)_2Ta(H)(H')_2$
	6.61	2	m	$HTa(\mu\text{-}\mathit{H})_2Ta(H)(H')_2$
	5.51	1	t, $^2J_{HH}$ = 5 Hz	$HTa(\mu\text{-}H)_2Ta(\mathit{H})(H')_2$
	3.25	2	broad s[c]	$HTa(\mu\text{-}H)_2Ta(H)(\mathit{H}')_2$

[a] Spectra obtained at 500 MHz. The −70 °C spectrum was resolution enhanced to observe small coupling constants. Chemical shifts are reported in δ, referenced to either Me_4Si or the residual protons in the solvent. [b] 250-Hz full width half-height. [c] 18-Hz full width half-height.

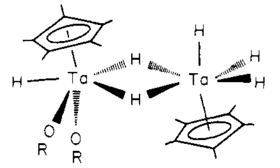

Figure 8. Structure proposed for $Cp^{*}(Me_3CO)_2HTa(\mu\text{-}H)_2TaH_3Cp^{*}$ (**7**).

The formation of **7** shows one of the difficulties in preparing coordinatively unsaturated hydride complexes of the early transition metals. These compounds have a strong tendency to form oligomers with bridging hydrogen atoms, indicating that the hydrides in these complexes are good ligands for other metal centers (cf. BH_4^-). For example, Cp_2TaH_3 strongly binds Lewis acids like $AlEt_3$,[26] Cp_2ZrH_2 is oligomeric,[27] and $(\eta^5\text{-}C_5H_4Me)_2ZrH_2$ is dimeric.[28] The hydride bridges in **7** are sufficiently stable to resist cleavage by excess trimethylphosphine.

Conclusions

High-field proton NMR spectroscopy has permitted the assignment of the coordination geometries for polyhydride complexes in the series $Cp^{*}ML_2H_3X$ (M = Nb, Ta). The hydride ligands appear in the NMR spectra in a 2:1:1 (X = H) or 2:1 (X = Cl) ratio, and the phosphorus atoms are equivalent when L is a monodentate phosphine. These data imply a C_s symmetry for these molecules; the structures are viewed as derived from a tricapped-trigonal-prism geometry (Figure 4a,b). The conclusions are supported by an X-ray crystal structure determination for $Cp^{*}Ta(PMe_3)_2H_4$, in which only the heavy atoms were located. The hydride complexes with a bidentate dmpe ligand—$Cp^{*}M(dmpe)H_4$—adopt a different structure: a C_s geometry with *in*equivalent phosphorus atoms (Figure 4c), presumably due to the constrained P–Ta–P angle.

---

(23) (a) The presence of both *tert*-butoxide ligands on one tantalum atom is also supported by the IR spectrum of **7** (Experimental Section). The CO stretch (assigned by following ref 25b, pp 116–122) appears at 1020 cm^{-1} in the IR spectrum of $Cp^{*}TaMe_3(OCMe_3)$, but two bands are present in this region (990 and 965 cm^{-1}) in the spectrum of **7**. Similar bands are observed in a number of mono- and dialkoxide complexes of tantalum.[23b] (b) Mayer, J. M.; Curtis, C. J.; Bercaw, J. E. *J. Am. Chem. Soc.*, in press.

(24) The other possible symmetry elements for $Cp_2^{*}Ta_2H_6(OCMe_3)_2$ can be ruled out as follows. An inversion center is clearly impossible because of the inequivalence of the Cp* groups. A twofold rotation axis would require a linear ring-centroid–tantalum–tantalum–ring-centroid arrangement, which leaves no place for the two unique hydride ligands.

(25) (a) Both alkoxide and hydride ligands are known to bridge metal centers readily.[7,25b] (b) Bradley, D. C.; Mehrotra, R. C.; Gaur, D. P. "Metal Alkoxides"; Academic Press: New York, 1978.

(26) Tebbe, F. N. *J. Am. Chem. Soc.* **1973**, *95*, 5412–14.

(27) Walles, P. C.; Weigold, H. *J. Organomet. Chem.* **1970**, *24*, 405–11.

(28) Jones, S. B.; Petersen, J. L. *Inorg. Chem.* **1981**, *20*, 2889–94.

The new dimeric hydride complex Cp*(Me$_3$CO)$_2$HTa(μ-H)$_2$TaH$_3$Cp* has also been examined, and its connectivity is clearly established from the NMR data. The molecule adopts an unusual asymmetric structure with two bridging hydride ligands.

Experimental Section

All manipulations were carried out with use of either high-vacuum or glovebox techniques, as previously described.[10] Potassium *tert*-butoxide (MCB) was sublimed and stored under nitrogen. ^{1}H NMR spectra were recorded on Bruker WM500 or JEOL FX90Q spectrometers; the spectra were frequently resolution enhanced[29] to observe small coupling constants. ^{31}P and ^{13}C NMR spectra were obtained with use of a JEOL FX90Q spectrometer. Infrared spectra were recorded on a Beckman 4240 spectrometer and are reported in cm^{-1}. Elemental analyses were determined by Alfred Bernhardt Analytical Laboratory. Molecular weights were determined either by osmometry (Bernhardt) or by isothermal distillation by the Singer method.[30]

Procedures. Cp*Ta(PMe$_3$)$_2$H$_4$ (1), Cp*Ta[P(OMe)$_3$]$_2$H$_4$ (2), Cp*Ta(PMe$_3$)$_2$H$_3$Cl (4), and Cp*Ta(dmpe)H$_4$ (5) have been previously reported.[10a] **Cp*Nb(PMe$_3$)$_2$H$_4$ (3)** and **Cp*Nb(dmpe)H$_4$ (6)** are prepared in a manner analogous to that for the tantalum compounds; full details will be published.[10b]

Cp*TaMe$_3$(OCMe$_3$). A solution of Cp*TaMe$_3$Cl[31] (3.1 g) and KOCMe$_3$ (0.88 g) in 75 mL of diethyl ether was stirred at −80 °C for 1 h and then warmed to room temperature. The diethyl ether was removed, and 20 mL of petroleum ether was added; the slurry was filtered into a sublimator and the solvent removed. Sublimation (10^{-3} torr) at 80 °C onto a probe at 0 °C yielded 2.4 g (71%) of yellow Cp*TaMe$_3$(OCMe$_3$). ^{1}H NMR (34 °C, C$_6$D$_6$): δ 1.75 (s, 15 H, Cp*); 1.24 (2, 9 H, OC(CH$_3$)$_3$); 0.43 (s, 9 H, Ta(CH$_3$)$_3$). ^{13}C NMR (34 °C, C$_6$D$_6$): δ 115.35 (s, C_5Me$_5$); 11.11 (q, J_{CH} = 127 Hz, C$_5$(CH$_3$)$_5$); 82.66 (s, OCMe$_3$); 52.51 (q, J_{CH} = 121 Hz, Ta(CH$_3$)(CH$_3$)′$_2$); 47.57 (q, J_{CH} = 118 Hz, Ta(CH$_3$)(CH$_3$)′$_2$); 30.61 (q, $^1J_{CH}$ = 126 Hz, OC(CH$_3$)$_3$; each peak of the quartet is split further into a septet, $^3J_{CH}$ = 4 Hz). IR: 1360, 1240, 1185 (s), 1020 (s), 790, 460. Molecular weight (C$_6$H$_6$): calcd, 434; found, 520 (Singer method).

Cp*(Me$_3$CO)$_2$HTa(μ-H)$_2$TaH$_3$Cp* (7). A high-pressure reactor, charged with 2.12 g of Cp*TaMe$_3$(OCMe$_3$), 0.8 mL of PMe$_3$, and 120 mL of petroleum ether, was heated to 65 °C, pressurized to 1400 psi of hydrogen gas, and then stirred for 1 week. The solvent was removed, leaving a brown oil containing principally **7**. After repeated additions and removals of petroleum ether, 0.9 g (43%) of white crystalline **7** was obtained. **7** is extremely soluble in hydrocarbon solvents, and it decomposes in vacuo at 135 °C. The ^{1}H NMR data is given in Table III. IR: 1735, 1535, 1280 (TaH; TaD: 1250, 1110, 860), 1360, 1240, 1185 (s), 990(s), 965(s), 790, 540 (TaOCMe$_3$), 1030 (Cp*). Anal. Calcd for C$_{28}$H$_{54}$O$_2$Ta$_2$: C, 42.86; H, 6.94; Ta, 46.12. Found: C, 42.66; H, 6.70; Ta, 46.33. Molecular weight (C$_6$H$_6$): calcd, 785; found, 760 (Bernhardt). **7** can also be prepared by stirring a solution of Cp*Ta(PMe$_3$)$_2$H$_3$Cl (**4**) and KOCMe$_3$ in diethyl ether for 30 min.

X-ray Data Collection. Crystals of Cp*Ta(PMe$_3$)$_2$H$_4$ (**1**) were obtained by cooling a petroleum ether solution. A crystal, roughly 0.11 × 0.13 × 0.20 mm, was mounted in a glass capillary under a nitrogen atmosphere. A series of oscillation and Weissenberg photographs revealed Laue symmetry no higher than $\bar{1}$. Lattice constants were obtained by a least-squares refinement of the orientation matrix with 15 reflections ($18 < 2\theta < 25°$), which were centered on a locally modified P2$_1$ diffractometer with graphite monochromator and Mo Kα radiation (λ = 0.71069 Å): a = 8.581 (2) Å, b = 14.244 (4) Å, c = 17.267 (4) Å, α = 90.34 (2)°, β = 99.96 (2)°, γ = 90.05 (2)°, V = 2079 Å^3, $P\bar{1}$, Z = 4.

A total of 8886 reflections ($+h,\pm k,\pm l$) were collected to a maximum 2θ of 40° in two shells, including sets of 3 check reflections measured after each block of 97 reflections, yielding 3904 unique reflections. No decomposition was observed. Intensities were measured by θ–2θ scans at a constant scan speed of 2.02° min^{-1}, angular dispersion correction to a fixed symmetric scan width of 2.0° in 2θ, and two stationary-counter, stationary-crystal background counts, each half the scan time, taken at the ends of the scan range. The data were corrected for Lorentz and polarization effects but not for absorption (μ = 54 cm^{-1}). Observational variances, $\sigma^2(F_o^2)$, were based on counting statistics plus the term $(0.02S)^2$, where S is the scan count.

Table IV. Fractional Atomic Coordinates (×10^5 for Ta, ×10^4 for All Others) and U_{eq} (×10^4 for Ta, ×10^3 for All Others)

	x	y	z	U_{eq},[a] Å^2
Ta(1)	48082 (8)	22268 (4)	13026 (4)	440 (2)
C(1A)	2363 (17)	2618 (12)	399 (8)	53 (7)
C(2A)	2390 (20)	1655 (11)	536 (11)	64 (6)
C(3A)	2303 (19)	1447 (11)	1318 (11)	60 (5)
C(4A)	2260 (20)	2347 (14)	1695 (10)	71 (6)
C(5A)	2355 (19)	3056 (10)	1120 (10)	57 (5)
C(M1A)	2182 (23)	3194 (14)	−333 (11)	87 (6)
C(M2A)	2205 (24)	943 (14)	−159 (13)	99 (7)
C(M3A)	1945 (24)	485 (13)	1584 (13)	93 (7)
C(M4A)	1941 (24)	2469 (25)	2511 (12)	94 (7)
C(M5A)	2126 (23)	4062 (12)	1325 (12)	88 (7)
P(1A)	6052 (6)	1105 (3)	2365 (3)	63 (1)
C(11A)	8138 (29)	1379 (18)	2784 (49)	135 (9)
C(12A)	6244 (35)	−102 (14)	2134 (12)	132 (9)
C(13A)	5354 (31)	1028 (16)	3289 (12)	120 (8)
P(2A)	6354 (6)	2519 (3)	205 (3)	62 (1)
C(21A)	6801 (26)	3722 (13)	−13 (12)	93 (6)
C(22A)	5653 (25)	2050 (14)	−794 (10)	89 (6)
C(23A)	8305 (23)	1978 (15)	375 (11)	94 (7)
Ta(2)	84057 (8)	69749 (4)	34832 (4)	417 (1)
C(1B)	10993 (19)	6782 (12)	3075 (11)	62 (6)
C(2B)	11103 (19)	6415 (10)	3869 (9)	49 (4)
C(3B)	10879 (19)	7198 (13)	4341 (9)	61 (6)
C(4B)	10633 (20)	8027 (11)	3864 (11)	63 (6)
C(5B)	10678 (19)	7758 (10)	3094 (9)	53 (5)
C(M1B)	11358 (24)	6214 (12)	2391 (10)	80 (6)
C(M2B)	11614 (21)	5487 (11)	4178 (11)	73 (6)
C(M3B)	11129 (24)	7182 (15)	5220 (11)	97 (7)
C(M4B)	10608 (26)	9028 (13)	4138 (14)	102 (8)
C(M5B)	10612 (24)	8366 (13)	2413 (12)	93 (6)
P(1B)	6759 (6)	7639 (3)	4437 (3)	69 (1)
C(11B)	7370 (28)	8659 (15)	5038 (14)	125 (8)
C(12B)	6200 (33)	6864 (15)	5176 (14)	131 (8)
C(13B)	4838 (28)	8093 (17)	3994 (16)	132 (9)
P(2B)	7306 (6)	5436 (3)	2873 (3)	57 (1)
C(21B)	8545 (26)	4447 (13)	2756 (15)	119 (9)
C(22B)	5915 (26)	4849 (13)	3394 (12)	94 (6)
C(23B)	6046 (28)	5463 (14)	1878 (9)	102 (8)

[a] $U_{eq} = {}^1\!/_3\Sigma_i\Sigma_jU_{ij}a_i^*a_j^*a_ia_j$; $\sigma(U_{eq}) = (U_{eq}/[3(6^{1/2})])\Sigma_i[\sigma(U_{ii})/U_{ii}]$.

Structure Determination and Refinement. The two tantalum atomic positions were derived from the Patterson map. An electron density map based upon these two atoms revealed all other non-hydrogen atoms. Atomic scattering factors were taken from Stewart et al.[32] for H and ref 33 for all others; the real part of the anomalous dispersion correction was applied to the Ta and P scattering factors.

Several cycles of full-matrix least-squares refinement minimizing $\sum w(F_o^2 - F_c^2)^2$, $w = \sigma^{-2}(F_o^2)$ on all non-hydrogen atom parameters yielded R_F = 0.059 (3715 reflections with $F_o^2 > 0$) and GOF = 4.31; all the atomic coordinates were in one matrix, and the scale factor, isotropic secondary extinction parameter, and anisotropic Gaussian amplitudes in the other. Hydrogen atoms (but not the hydride ligands) were introduced into the model as revealed by idealized geometry and difference maps, with a fixed isotropic B = 8 Å^2. Several additional cycles of least-squares refinement, with fixed hydrogen atoms, converged with R_F = 0.056 and GOF = 3.91.

Examination of the final difference Fourier maps revealed a number of peaks (height > 0.4 e/Å^3) that represented reasonable possibilities for the positions of the hydride ligands, based on the idealized geometries discussed above and normal Ta–H bond lengths.[7] However, these atoms did not refine properly when included in the least-squares refinement. Thus, we were not convinced that the positions of any of the hydride ligands could be assigned from this X-ray data set.

---

(29) Ernst, R. R. *Adv. Magn. Reson.* **1966**, *2*, 1.

(30) (a) Singer, R. *Justus Liebigs Ann. Chem.* **1930**, *478*, 246. (b) Clark, E. P. *Ind. Eng. Chem., Anal. Ed.* **1941**, *13*, 820.

(31) McLain, S. J.; Wood, C. D.; Schrock, R. R. *J. Am. Chem. Soc.* **1979**, *101*, 4558–70.

(32) Stewart, R. F.; Davidson, E. R.; Simpson, W. T. *J. Chem. Phys.* **1965**, *42*, 3175–87.

(33) "International Tables for X-Ray Crystallography"; Kynoch Press: Birmingham, England, 1974; Vol. IV, pp 71–98.

Fractional atomic coordinates and U_{eq}'s are given in Table IV.

Acknowledgment. We acknowledge the help and advice of Bill Croasmun, the use of the Southern California Regional NMR Facility, and the support of the NSF Grant No. 7916324A1. We also thank Richard E. Marsh and William P. Schaefer for sage counsel and Sten Samson for his help in the development and improvement of our X-ray diffraction facility. This work has been supported by the National Science Foundation Grant No. CHE8024869.

Registry No. **1**, 80964-80-3; **2**, 80964-82-5; **3**, 84849-47-8; **4**, 80964-84-7; **5**, 80964-83-6; **6**, 84849-48-9; **7**, 84849-49-0; Cp*TaMe$_3$(OCMe$_3$), 84849-50-3; Cp*TaMe$_3$Cl, 69302-75-6; KOCMe$_3$, 865-47-4.

Supplementary Material Available: Listings of fractional atomic coordinates for hydrogen atoms (Table V), anisotropic Gaussian amplitudes for nonhydrogen atoms (Table VI), and structure factor amplitudes (Table VII) and a stereoscopic drawing of a unit cell of Cp*Ta(PMe$_3$)$_2$H$_4$ (**1**) (Figure 9) (23 pages). Ordering information is given on any current masthead page.

Contribution from the Department of Chemistry,
University of Sheffield, Sheffield S3 7HF, England

Comparison of the Crystal and Molecular Structures of Cyclopentadienylbromodicarbonylruthenium(II) and (Ethyltetramethylcyclopentadienyl)bromodicarbonylruthenium(II)

HARRY ADAMS, NEIL A. BAILEY,* and COLIN WHITE*

Received July 9, 1982

The crystal structures of Ru(η-C$_5$H$_5$)(CO)$_2$Br (monoclinic, a = 9.807 (7) Å, b = 7.023 (3) Å, c = 13.436 (11) Å, β = 106.83 (6)°, Z = 4, $P2_1/c$, R = 0.0462) and Ru(η-C$_5$Me$_4$Et)(CO)$_2$Br (monoclinic, a = 6.980 (6) Å, b = 11.419 (9) Å, c = 9.205 (8) Å, β = 95.32 (7)°, Z = 2, $P2_1/m$, R = 0.0460) show that the molecules adopt rotationally different conformations but otherwise exhibit similar bond lengths for their common skeleton. The former has an ordered, delocalized cyclopentadienyl ring positioned so that one carbon atom closely eclipses the bromo ligand. In contrast, the latter molecule, which has crystallographically imposed C_s symmetry, adopts a staggered conformation with the ring carbon carrying the ethyl substituent trans with respect to the bromide; partial bond localization was also observed within the alkylated ring. A possible relationship between the structural differences and the different reactivities of these two compounds is commented upon.

Introduction

The chemistry of cyclopentadienyl–metal complexes is one of the cornerstones of organometallic chemistry. Over the last 15 years, however, chemists have turned in increasing numbers to the use of pentaalkyl-substituted cyclopentadienyl ligands, which display several desirable features compared to their unsubstituted cyclopentadienyl analogues. For example, they normally exhibit considerably longer catalytic lifetimes as is the case for the oligomerization catalysts [Y(η^5-C$_5$Me$_4$Et)$_2$-n-Bu][1] and [Ta(η^5-C$_5$Me$_5$)Cl$_2$(1-octene)].[2] In addition, the chemical reactivity is often very different from that of the corresponding cyclopentadienyl complexes; thus, [Mo(η^5-C$_5$Me$_5$)$_2$] readily reacts with hydrogen or carbon monoxide but [Mo(C$_5$H$_5$)$_2$]$_n$ is relatively inert.[3] Similarly, whereas the protonated form of the duroquinone complex [Co(η^5-C$_5$H$_5$)(η^4-C$_6$Me$_4$O$_2$)] has only been observed in strong acid solution, the corresponding protonated complex [Co(η^5-C$_5$Me$_5$)(η^6-C$_6$Me$_4$(OH)$_2$)](BF$_4$)$_2$ may be isolated.[4]

Comparative chemical and structural studies on related compounds have proved to be invaluable in advancing chemical knowledge. For example, such studies on the various effects of changing the nature of the substituents on phosphorus donor ligands have contributed significantly to an understanding of organometallic reactions.[5] Unfortunately, there have been few systematic attempts to compare the structures and properties of peralkyl-substituted and unsubstituted cyclopentadienyl complexes. Obviously peralkyl-substituted cyclopentadienyl ligands are larger and better electron donors than C$_5$H$_5$ ligands, but to what extent these features influence the properties of particular metal complexes remains largely a matter of chemical intuition. As a contribution to understanding such factors we report and compare the crystal structures of Ru(Cp′)(CO)$_2$Br (Ia, Cp′ = C$_5$H$_5$; Ib, Cp′ = C$_5$Me$_4$Et). These two complexes were chosen for comparison because they exhibit distinct differences in their chemical properties. Thus, unlike the C$_5$H$_5$ analogue, Ru(η^5-C$_5$Me$_4$Et)(CO)$_2$Br is oxidized by bromine to the corresponding ruthenium(IV) complex, Ru(η^5-C$_5$Me$_4$Et)(CO)Br$_3$.[6] Equally important is the fact that the relative reactivities of these two

Table I. Atomic Positional Parameters with Estimated Standard Deviations for Ru(C$_5$H$_5$)(CO)$_2$Br

	x/a	y/b	z/c
Ru(1)	0.24295 (12)	0.02824 (18)	0.22844 (8)
Br(1)	0.19798 (21)	0.37325 (28)	0.17290 (14)
O(1)	0.3736 (13)	−0.0500 (20)	0.0557 (8)
O(11)	−0.0495 (13)	−0.0853 (22)	0.0941 (8)
C(1)	0.3228 (15)	−0.0190 (26)	0.1182 (11)
C(2)	0.3823 (22)	−0.1644 (30)	0.3365 (11)
C(3)	0.4353 (16)	0.0163 (32)	0.3669 (11)
C(4)	0.3338 (19)	0.1123 (28)	0.3969 (10)
C(11)	0.0631 (16)	−0.0349 (28)	0.1442 (11)
C(12)	0.2470 (24)	−0.1850 (29)	0.3507 (13)
C(13)	0.2153 (19)	−0.0136 (32)	0.3859 (11)

---

[1] D. G. Ballard, A. Courtis, J. Holton, J. McMeeking, and R. Pearce, *J. Chem. Soc., Chem. Commun.*, 994 (1978).

[2] S. J. McLain, J. Sancho, and R. R. Schrock, *J. Am. Chem. Soc.*, **101**, 5451 (1979).

[3] J. L. Thomas, *J. Am. Chem. Soc.*, **95**, 1838 (1973).

[4] G. Fairhurst and C. White, *J. Chem. Soc., Dalton Trans.*, 1531 (1979).

[5] C. A. Tolman, *Chem. Rev.*, **77**, 313 (1977).

[6] I. W. Nowell, K. Tabatabaian, and C. White, *J. Chem. Soc., Chem. Commun.*, 547 (1979).

0020-1669/83/1322-1155$01.50/0